AD-A080 427 MASSACHUSETTS INST OF TECH LEXINGTON LINCOLN LAB F/G 20/3
INTERMODULATION MEASUREMENT IN THE UHF BAND AND AN ANALYSIS OF --ETC(U)
NOV 79 J C LEE F19628-80-C-0002
UNCLASSIFIED TN-1979-70 ESD-TR-79-269 NL

1 OF 1

AD
A080427

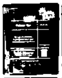

END
DATE
FILMED
3-80
DDC

(12)

MASSACHUSETTS INSTITUTE OF TECHNOLOGY

LINCOLN LABORATORY

(6)

INTERMODULATION MEASUREMENT IN THE UHF BAND AND AN ANALYSIS OF SOME BASIC CONDUCTING MATERIALS,

(10) Joseph C./LEE
Group 61

(14) TN-1979-70

(9) TECHNICAL NOTE 1979-70

(11) 19 NOV[redacted]79 (12) 48

(15) F19628-80-[illegible]-[illegible] (18) ESD

(16) 2149 (19)

Approved for public release; distribution unlimited. TR-79-267

LEXINGTON MASSACHUSETTS

207650

ABSTRACT

In a modern communications satellite, it is generally required that high-power multi-channel transmitters and super-sensitive broadband receivers be packed in a limited space. Because of the very large power level difference between the transmit and receive signals and the limitation of frequency allocation, intermodulation (IM) interference due to passive residual nonlinearities in the high-power transmission path can be a real problem. This kind of problem did crop up during several communication satellite development programs.

The work reported here represents ~~some~~ of ~~our~~ effort~~s~~ toward a better understanding of the general IM phenomenon. Passive nonlinearities of resistivity in conducting material, in contrast with that due to contact junctions, were studied by careful measurement and analysis. Forward and backward traveling wave IM's in a long transmission line were distinguished and interpreted. New evidence concerning the deviation from Ohm's law by metal conductors was obtained and quantitative characterization of the weak nonlinear characteristics of good conductors was attempted. The IM production of steel, stainless steel, and graphite fiber were conclusively demonstrated. These materials are used in certain filter and antenna fabrications in aerospace applications for low thermal expansion or light weight.

CONTENTS

LIST OF ILLUSTRATIONS

LIST OF TABLES

I. INTRODUCTION

Absolute linearity exists only in the abstract world. In the real world, it can provide a good model of the first approximation for certain relations over some ranges and with some nonlinearity tolerances. At the beginning, many fundamental laws of physics start with a linear relation. Hooke's law on elastic properties of solids, Newton's second law of motion, and Ohm's law for electric conductors are three prominent examples. In all of these cases, the linear relations are only empirical approximations with limitations to their accuracy and range of application. Each may be regarded as the first term in a Taylor's expansion of the function relationship between the two variables. Thus, it is inevitable that a supposedly linear system will shown some non-linear effects when pushed too far or looked at too closely.

It is well known that over the elastic limit, the Hooke's law breaks down and the material under test will suffer permanent set. If the applied stress is further increased the test sample will finally break. The failure of linearity of Newton's second law has the most significance in the introduction of relativistic effects into the laws of motion. The breakdown of Ohm's law is less spectacular but nevertheless has important significance. Many materials are found not to obey Ohm's law exactly. They are called non-Ohmic of which semiconductors[1] and plasmas[2] are two important classes.

In electromagnetic theory, Maxwell's equations are linear but the constitutive equations which describe the electromagnetic macroscopic properties of matter may be nonlinear. Nonlinear materials may generate harmonics and intermodulations in an intended (mixers, limiters) or unintended fashion in a communication system. The latter case is called harmonic and intermodulation interference.

The first indication of such an interference was noticed in 1934 in Europe. It is called the Luxembourg effect. The amplitude modulation of the Luxembourg station (long wave and high power) was noticed in Holland on the frequencies of some broadcast stations. This nonlinearity was later attributed

efforts to reduce it may be directed to the wrong place. Hit-and-miss tactics to combat IM are likely to be inefficient and costly. The work reported here represents some of our efforts toward a better understanding of the general IM phenomenon.

Existing IM studies were limited to the more obvious possible nonlinearities such as: contacts[6], diodes[7], ferromagnetic[8] and ferrite materials[9], and ferroelectric materials. The work reported here will include some measured IM levels generated by many commonly used conducting materials (copper, aluminum, brass, stainless steel, cold-rolled steel, graphite, etc.). The measurements are in the UHF band. Contact nonlinearity at the most critical locations in the measurement is avoided by the use of quarter-wavelength couplings. One important conclusion of the work is that conducting materials do generate IM's. Graphite materials and magnetic materials can generate very high levels of IM's. Some IM analysis based on nonlinear conductivity (or permeability) are attempted. IM's generated in rf cables both of braided and solid conductor types were measured and analyzed based on uniformly distributed nonlinearities. Measured differences in transmitted and reflected IM levels were explained by a traveling-wave IM generation mechanism.

II. MEASUREMENT AND ANALYSIS

1. Measurement Setup

A block diagram of the IM measurement setup used in the present work is given in Figure 1. Two channel transmitting signals (f_1 = 245 MHz, f_2 = 268 MHZ) originated from frequency synthesizers are amplified by separate power amplifiers to give an output of 44 dBm (25 watts) per channel. They are combined through a network of hybrids and filters in the transmit screen room and are then sent to the transmit port of the input test diplexer. The component under test (CUT) is connected between the two common ports of the two (input and output) test diplexers. The transmitted and reflected IM's are measured from the receive ports of the two diplexers with a spectrum analyzer. Using a low noise amplifier (NF = 2 dB) in front of the spectrum analyzer and with the IF bandwidth of the analyzer set to 10 Hz, the practical limit of a detectable signal is about -160 dBm.

The third order IM at frequency $2f_2 - f_1$ = 291 MHz, and the fifth order IM at frequency $3f_2 - 2f_1$ = 314 MHz were measured. The 7th order IM cannot be measured readily due to the receive frequency band limitations of the test diplexers. It is generally agreed that power level in IM decreases as the IM order increases and that the third order IM is the strongest interference source. For this reason we have concentrated our attention on the third order IM. Unless stated otherwise, the word IM is used to mean the third order IM.

The IM level at the output port of the power-combining network was about -80 dBm. The isolation between the transmit and receive ports of the test diplexers at the IM frequency was about 86 dB. Thus the contribution of IM level due to leakage through the test diplexer was limited to about -166 dBm. This level was negligble compared to IM levels generated at the common port connector of the test diplexer. The measured test diplexer IM level with its common port open circuited was between -120 to -133 dBm. Under well matched conditions, the residual IM level of the test diplexer seemed to be limited by the TNC connectors used in the common ports. The lowest IM levels were measured between -120 to -125 dBm using silverplated brass TNC male to male adapters.

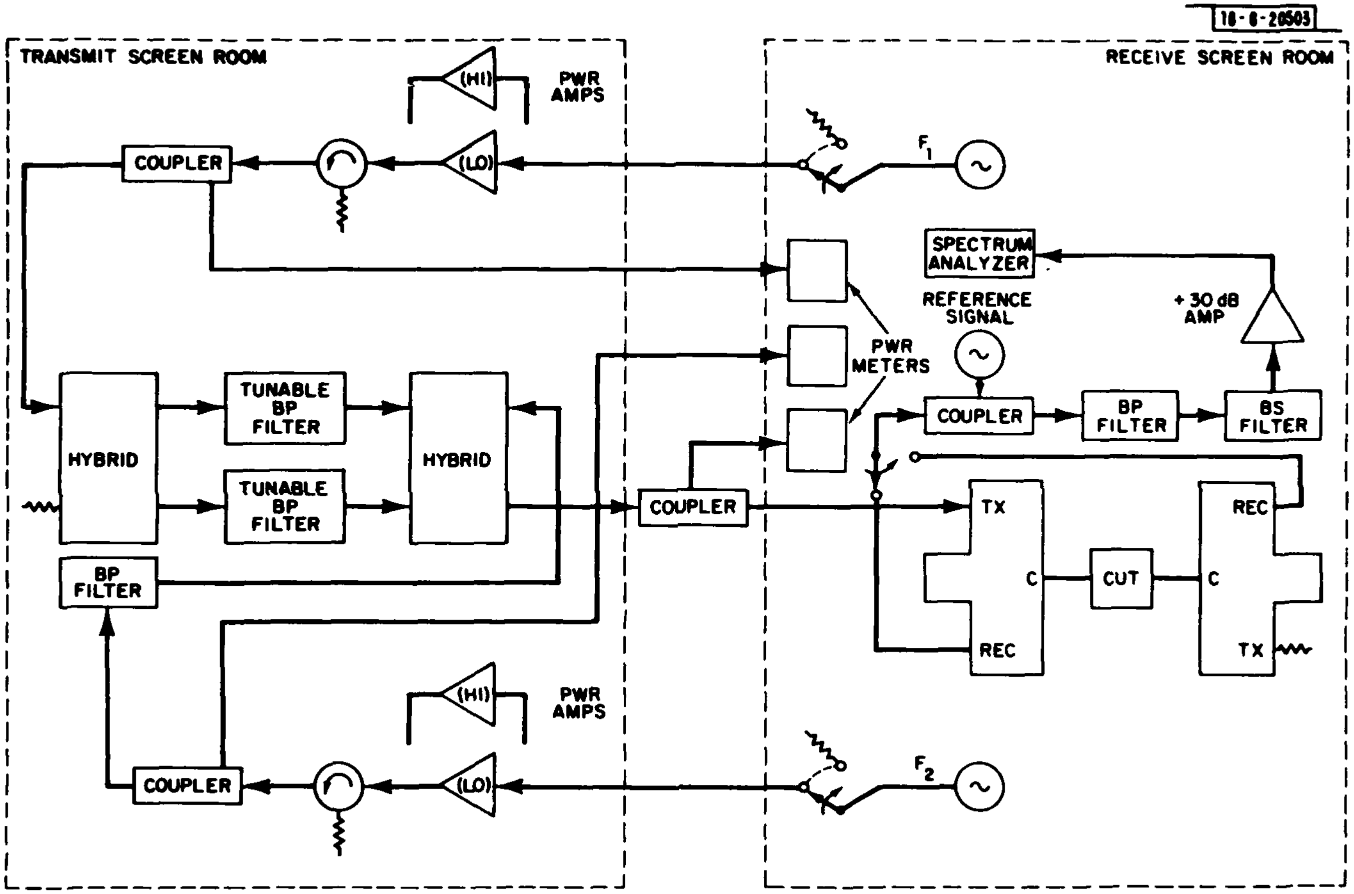

Fig. 1. Block diagram of the IM measurement setup.

The test diplexers were of interdigital design made of aluminum with dimensions of about 24 inches x 12 inches x 1.5 inches. The contact of the resonant rods and the diplexer cover to the diplexer body were carefully designed to ensure a pressure of about 10,000 psi. The diplexer interior was polished to about 4-8 microinch finish. Each diplexer weighed about 38 pounds. Due to the heavy weight of the diplexer and the rather delicate construction of the connectors used, the two test diplexers were fixed onto two x-y drives on a flat table to permit good alignment of their connectors in connecting them together.

2. Connectors

Various commercially available TNC adaptors of different sex combinations were measured. The results showed consistently that the surface material used in the connector is an important factor affecting IM levels. It seems contact, conductivity and magnetic properties of the surface material are all important. Typical IM levels are summarized in Table I.

TABLE I

MEASURED IM LEVELS OF TNC ADAPTORS

Body Material	Surface Material	Reflected 3rd Order IM Level in dBm
Brass	Silver Plated	-120 to -125
Aluminum	Electroless Nickel Plated	-117 to -130
Brass	TR-5* Finish	-90 to -111
Stainless Steel	Stainless Steel	-88 to -105

From Table I we see that connectors with stainless steel surface finish generated highest level IM's which confirms other measurement results[9]. Stainless steels are ordinarily considered "nonmagnetic". But this nonmagnetic property is not absolute. Under annealed conditions their permeability is listed to be 1.02. Under stress this value could be much higher. This is evidenced

*TR-5 is a trade name of Kings Electronics Co., Inc. for a surface finish.

by the fact that a small magnet can pick up a small stainless steel washer. Not known is the relative importance of the contact between two hard surfaces and the nonlinear magnetic properties in contributing to high IM generation.

The next highest IM contributer is TR-5. This finish appears to involve layers of plating on brass, including copper, zinc and nickel, a total of less than 1 mil* in thickness. At the frequency range used, the skin depth for good conducting material is in the 0.2-0.3 mil range; thus all three layers may have influence on the overall IM level. It is not clear how much IM is contributed by the hard copper-zinc layer through poor contact and how much by the nickel layer through non-linear magnetic property.

In electroless nickel plating[10] nickel-phosphorous alloys are formed. These alloys have a higher electrical resistance than that of nickel. If the deposits contain phosphorus in excess of 8 percent the alloy is then "nonmagnetic"[11]. This property of electroless nickel plating may be the reason for lower IM levels for the electroless nickel as compared to the TR-5.

Similar tests of type N connectors yielded similar results. We found gold plated connectors usually work as well as silver plated ones. Due to their larger size, type N connectors are expected to have lower IM than TNC types. However, since the TNC connectors in the test diplexers always form part of the component under test (CUT), this conviction cannot be demonstrated. However, for low IM components we always use silver or gold plated connectors. Limited tests on GR-900 gold plated connectors showed an IM level of -120 dBm.

3. Cables

Many existing cables with different connectors and specially made cables with selected connectors were tested. We found that for most cables the measured reflected IM levels are dominated by the connectors used. One important IM source was found at the cable outer conductor contact with the connector body. Mechanical support in this area is important. The IM level could be very sensitive to any movement or vibration in this area. Some typical ranges of IM levels are given in Table II.

*1 mil = .001 inch = .0025 cm.

TABLE II

MEASURED IM LEVELS OF COAXIAL CABLES

Cable Description	Connector	Center Pin	Outer Conductor	Reflected 3rd Order IM Level (dBm)
RG 214/u	TNC	gold plated	gold plated	-90 to -122
	N	" "	nickel plated	-95 to -100
	N	silver plated	silver plated	-120 to -127
	N	copper plated	copper plated	-132 to -138
0.141" semi rigid	SMA solder	gold plated	gold plated	-105 to -110
	SMA crimp	" "	" "	-108
	TNC	silver plated	silver plated	-123 to -132
RG 58/u	TNC	gold plated	nickel plated	-66 to -113

From the table we see that RG 214/u or 0.141 inch semirigid lines can be made with low reflected IM (below -120 dBm) by careful selection of connectors and following good cabling procedure. It is clear that a long length of such a cable with an insertion loss of 10 dB or more can be used as a low IM load.

Several RG-214/u cables with low-IM connectors were made. Both the forward (transmitted) and backward (reflected) IM characteristics were measured. Each cable was measured both ways to screen out any bad connectors or cables with questionable construction. After many iterations a careful selection of a set of cables of various lengths representing the best state-of-the-art for low IM was obtained. Intermodulation products from these cables were carefully measured. For cables of more than a few feet long, we found that in general:

(1) the reflected IM levels were lower than the transmitted IM levels,

(2) the reflected IM levels were not a strong function of the cable length as long as the cable was well matched with a low IM load,

(3) the transmitted IM level was a strong function of the cable length.

Some typical results for different lengths of RG-214/u cable are given in Table III. The third column is the 3rd order forward IM level relative to its maximum value in column 4.

The general trend of higher IM level in the forward direction than in the backward direction suggest that there may be a cumulative traveling wave IM generation effect. Neglecting the initial IM component in the forward direction at the input port of the cable, and assuming uniformly distributed nonlinearity in the parameters of the transmission line, the electric voltage of the accumulated forward nth order IM is given by

$$V_{IM_n} = K_n \left(e^{-\alpha_0 \ell} - e^{-n\alpha_0 \ell}\right) \tag{1}$$

$$K_n = A_n \frac{V_1^{n-1} V_2^{n-2}}{\alpha_0} \alpha_{n-1} \tag{2}$$

for $n = 3$, $A_n = \frac{3}{8}$.

TABLE III

TYPICAL MEASURED IM's FOR RG-214/u CABLES

Cable Length feet	Measured Attenuation dB	Relative IM_3 Level dB	IM_3 dBm		IM_5 dBm	
			Forward	Backward	Forward	Backward
4	-0.2	-11	-119	-129	-150	-144
16	-0.6	-9	-117	-124	-137	-148
20	-0.8	-7	-115	-123	-140	-142
63	-2.6	-1	-109	-122	-134	-144
127	-5.0	0	-108	-130	-135	-145
254	-9.8	-2	-110	-125	-137	-144
508*	-19.6	-9	-117	-119	-138	-142

RG-214/u cable has two layers of silver plated copper braids for outer conductor, solid polyethylene dielectric, and seven-strand silver plated copper inner-conductor.

*Four separate cables connected together with TNC connector adaptor

It is assumed that the zeroth order average attenuation constant at the two driving frequencies is α_0.

The derivation of the above relations for n=3 is given in Appendices B and C. Figure 2 is a plot of Eqn. (1) for the theoretical forward 3rd order IM levels. As the cable length increases from zero, the IM's will rise up from zero first linearly then saturate to a maximum level and then level off to zero slowly as the cable length approaches infinity. The conditions for maximum IM can be found exactly from Eqn. (1). For the 3rd and 5th order IM's, the conditions correspond to cable lengths with insertion loss of -4.8 dB and -3.5 dB respectively. Checking back with the measured data in Table III, we see the agreement to be good for the 3rd order and fair for the 5th order. Further deviation for measured higher-order IM's from theoretical values are expected due to their extremely low power level.

In previous studies, cables similar to RG-214/u in size were measured[12]. Length of the cables chosen were 0.5 m (1.6 feet), 1 m (3.3 feet) and 5 m (8.2 feet). The highest cable insertion loss tested in these studies is estimated by us to be 0.4 to 0.5 dB for the 5m cable. Thus, the cables tested were all well below the condition for maximum IM level (about 5 dB loss). It was observed that the longer the length of the cable, the higher the level of the IM's. Thus, measured results generally support this theoretical analysis.

In the past, the unwanted IM sources were almost universally attributed to current crossing a poor metallic contact in connectors and in the braids of flexible cables. With the differentiation of backward and forward IM's, we can separate IM's generated in the cable from those generated in the connectors. If cables without braids are used, we can determine if IM can be generated by other means than contact. Many 0.141 inch diameter semi-rigid cables with copper outer conductor, Teflon PTFE dielectric and silver plated copper inner conductor were made with silver-plated TNC connectors. As before, great care was used to reduce IM levels generated at the connectors. Some typical measured results are given in Table IV. The consistent difference

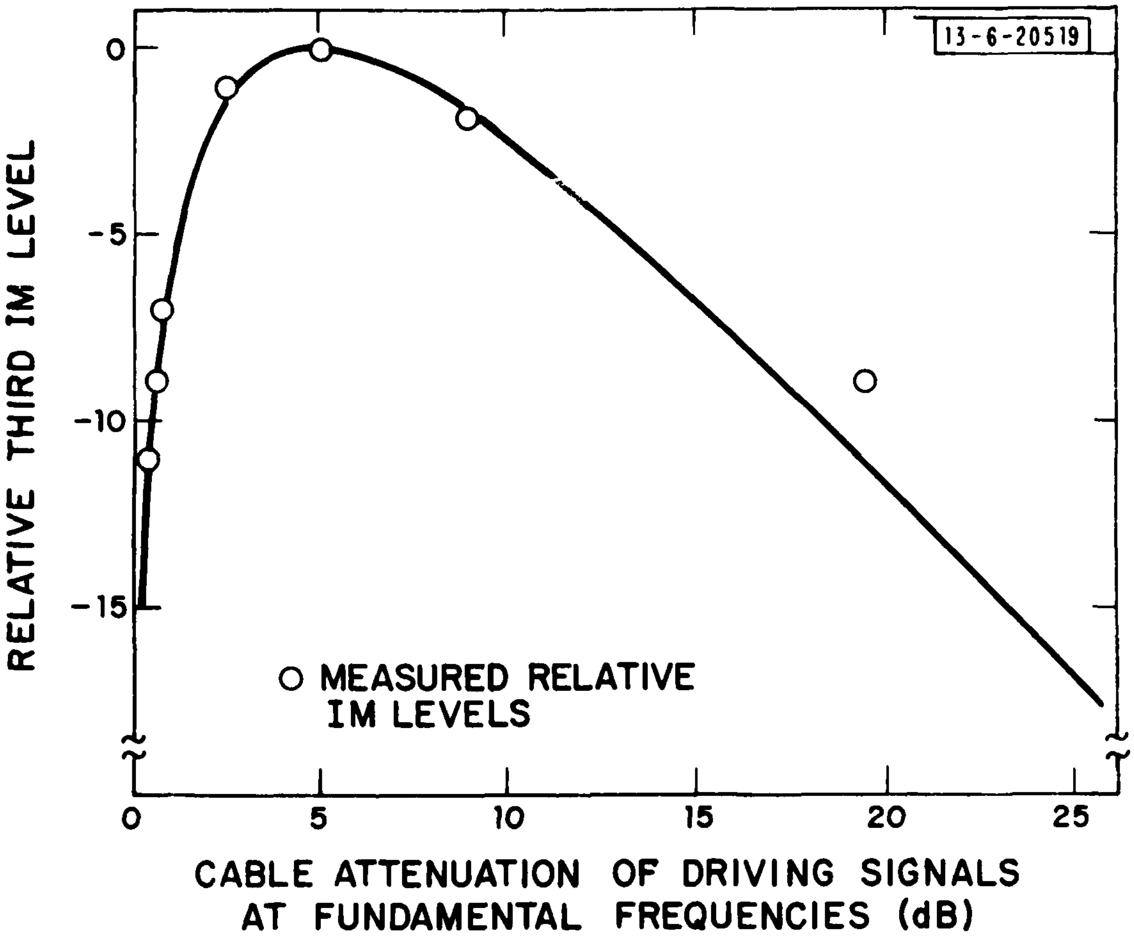

Fig. 2. Relative variations of the forward 3rd order IM level with cable length in terms of cable loss.

TABLE IV

TYPICAL MEASURED IM's FOR 0.141 INCH DIAMETER SEMI-RIGID CABLES

Cable Length inches	Measured Attenuation dB	IM_3		IM_5	
		Forward	Backward	Forward	Backward
4	0.02	-118	-129	-141	-145
5.5	0.02	-118	-127	-140	-143
20	0.09	-115	-135	-141	-135
600	-2.6	-111	-125	-130	-144

between forward and backward 3rd order IM's strongly suggest IM's are generated in the semi-rigid cable in a traveling wave parametric amplifier fashion. No maximum IM level was reached in the test due to the limitations of available cable length. This test showed that IM's may originate from causes other than metallic contacts or ferromagnetic materials. In fact, it showed that a coaxial cable made of solid good conductors like silver and copper and low-loss, temperature stable dielectric like Teflon did generate IM's. We may begin to suspect some kind of contamination due to metal chips on the metal inner surfaces or in the dielectric material. But such a localized culprit does not fit the measured IM characteristics which are more consistent with the analysis based on a uniformly distributed nonlinearity. At this point we have to ask the question: Can a good conductor or a good dielectric be non-linear and thus generate IM's? In the following paragraphs we will try to answer this question.

Some dielectric materials with very high dielectric constant like barium titanate are ferroelectric and are known to be nonlinear[13]. At ordinary field intensities, however, most dielectrics are considered to be linear. Efforts were made to find any indication of nonlinearity of Teflon and polyethelene in scientific books and journals. So far, none have been found.

Similar efforts were made for conductors. For a long time, it has been known that not all conductors are ohmic. An example of a non-ohmic conductor is thyrite[14] in which current is roughly proportional to the cube of voltage. Since Ohm's law was formulated in 1826, most textbooks on electricity have taken it for granted that metallic conductors are ohmic (their resistances are constant). However, some evidences of weak deviation from Ohm's law for metals were mentioned in a few places[14,15]. For most metals, little change in resistance occurs when current densities of up to 10^5 A/cm^2 are used. In the case of gold, there is no appreciable change in the resistivity for current densities as high as 10^6 A/cm^2 and a change of only a few percent at 10 times that current density*.

*However, another reference stated[16] "No deviation has ever been clearly demonstrated experimentally. According to one theoretical prediction, departures of the order of 1 percent might be expected at a current density of 10^5 A/cm^2."

Assuming there is 3 percent change in resistivity at current density of 10^7 A/cm^2 and that the nonlinear electric field-current density relation for gold can be simplified to the first two terms in a power series expansion (Appendix A):

$$E = \rho(J)\, J$$

$$= (\rho_0 + \rho_2 J^2) J = \rho_0 \left(1 + \frac{\rho_2}{\rho_0} J^2\right) J \quad . \qquad (3)$$

We have

$$\frac{\rho_2}{\rho_0} J^2 = 0.03 \; , \qquad \text{for } J = 10^7 \text{ A/cm}^2; \quad \text{or}$$

$$\frac{\rho_2}{\rho_0} = 3 \times 10^{-16} \text{ cm}^4/\text{A}^2 \quad .$$

For order of magnitude IM estimation for a RF cable, we will assume this same nonlinearity for other good conducting metals like silver and copper. The current density on the surface of the center conductor in a coaxial cable is:

$$J_m = \frac{I_m}{2\pi r_i \delta} \quad . \qquad (4)$$

If the cable has a 50 ohm impedance and carries 25 watts of power, $I_m = 1$ A. For 0.141 inch diameter semi-rigid cable $2r = 0.0359$ inch. For silver at 250 MHz $\delta = 1.6 \times 10^{-4}$ inch. We have

$$J_m = 8730 \text{ A/cm}^2 \quad .$$

The ratio of the 3rd order IM field to that of dissipation loss at the fundamental frequency is given by $\rho_2/\rho_0 \; J_m^{\;2} = 2.28 \times 10^{-8}$ or -156 dB in power level difference. For a two-tone signal at 25 watts at each frequency, the fundamental power level is 44 dBm per tone. A cable of about 19 feet long will have an insertion loss of 1 dB which corresponds to a dissipated power of 37 dBm and the 3rd order IM level is estimated to be -119 dBm, a significant level for satellite communications.

For the last case of Table IV (the measured forward 3rd-order IM level of -111 dBm and the insertion loss of 2.6 dB for the 600 inch long 0.141 inch diameter semi-rigid cable), the nonlinearity of the attenuation "constant" ratio may be calculated using Eqn. (1) with the result:

$$\frac{\alpha_2}{\alpha_0} = 1.44 \times 10^{-7} \; A^{-2} \; .$$

The nonlinearity in resistivity for the silver plated center conductor is related to that of the attenuation "constant" by the following relation (see Appendix A):

$$\frac{\rho_2}{\rho_0} = 2 \, \frac{\alpha_2}{\alpha_0} \, (2\pi\delta r_1)^2 = 2.9 \times 10^{-15} \; \mathrm{cm}^4/A^2 \; .$$

This is one order of magnitude higher than the estimated value based on Harnwell's[14] remarks about resistivity nonlinearity. Harnwell's book was written about 30 years ago. Because it is not clear how that resistivity nonlinearity was measured, we can not be sure how accurate that quoted value may be. But the fact that nonlinearity for good conductors derived from this IM measurement under numerous assumptions differs from the previous one by only one order of magnitude is quite amazing. The numerical accuracy of the nonlinear resistivity will definitely be improved by more and better measurement in the future. At present the fact of the existence of nonlinearity in resistivity of good conductors seems to be reinforced.

4. IM Measurement of Conducting Materials

To determine the IM levels due to different conducting materials, test samples made of various materials have to be put between the two test diplexers. To eliminate nonlinear contact impedance at the contact joints, a test fixture utilizing quarter wave coupling for the inner conductor of a large, rigid coaxial line was designed. Figure 3 is a sketch of the test fixture. The large, outer coaxial line with air dielectric has an outer conductor with ID = 0.563 inch and inner conductor with OD = 0.244 inch (characteristic impedance Z_0 = 50 Ω). The quarter wave coupling is accomplished by another coaxial line built inside the inner conductor. The test samples are made to form the inner conductor. For the inner coaxial line, the ID of the outer conductor is 0.200 inch and the OD of the inner conductor is 0.162 inch (characteristic impedance $Z_{0s} \approx 10\ \Omega$). The two conductors are separated by a commercially available Teflon tube of 0.024 inch wall thickness. The length of the inner conductor is chosen to be about two quarter wavelengths long at 250 MHz. The loaded Q of the resonant circuit is very low ($Q_L = \pi Z_{0s}/8Z_0 = 0.04$); the return loss at the driving (transmit) frequencies is greater than 20 dB and at the IM_3 (receive) frequency of interest is better than 15 dB. Test samples of 0.162 inch diameter and 23.125 inch long with rounded ends were made of various conducting materials. Their pertinent electrical parameters are listed in Table V. The measured 3rd order IM levels together with the calculated current density in the test sample and minimum insertion loss at resonance are given in Table VI. From Table VI, the following preliminary conclusions can be drawn:

(1) IM's generated in the forward and backward directions by standing waves have about the same level.

(2) Good conductors such as copper, aluminum, and brass have apparent 3rd IM levels about -120 dBm. The actual value may be lower, but the minimum measurable level may be limited by the TNC connectors between the test diplexers and the IM test fixture.

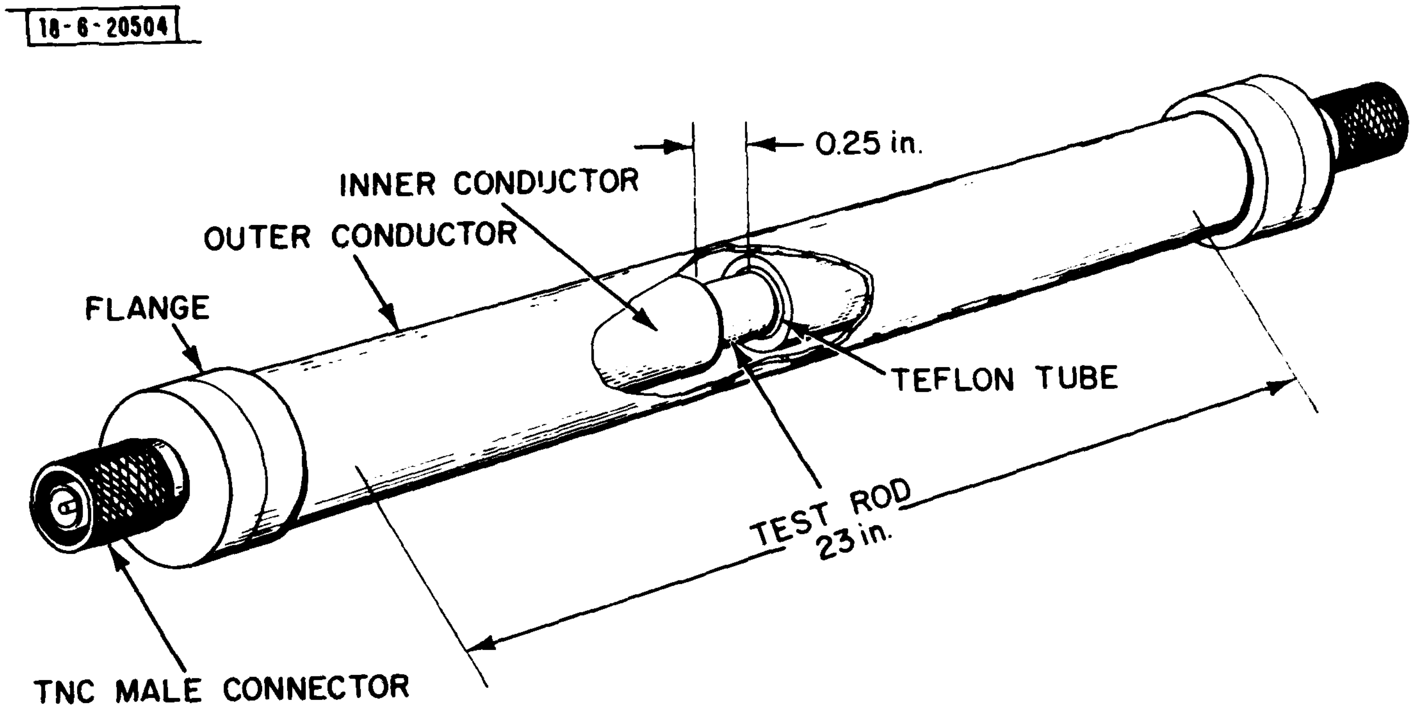

Fig. 3. Cross-sectional view of the conducting material IM test fixture.

TABLE V

PERTINENT ELECTRICAL PARAMETERS OF TESTED CONDUCTORS

Conductor	Conductivity at Room Temp. $\sigma x10^{-7}$ mohs/m	Relative Conductivity σ_r	Relative Permeability μ_r	Skin Depth at 250 MHz $\delta x10^{4}$ inches
Copper	5.8	1	1	1.64
Aluminum	3.7	0.63	1	2.07
Brass	2.3	0.4	1	2.59
Stainless Steel**	1.4	0.24	1.02 (annealed)	3.31
Graphite**	0.01	0.0017	1	39.5
Cold-Rolled Steel	1.0	0.17	180	0.30

*Type 303

**The graphite rod was "pultruded" (pulled from the processing equipment), and supplied by Columbia Products Co., Columbia, S. C. Hercules graphite fiber-AS with anhydride epoxy resin was used. All fiber orientation was unidirectional.

TABLE VI

MEASURED IM LEVEL AND INSERTION LOSS

Material	Forward IM_3 dBm	Backward IM_3 dBm	Calculated Current Density A/cm^2	Minimum Insertion Loss dB
Copper	-120	-118	1,857	0.05
Aluminum	-124	-121	1,471	0.05
Brass	-120	-122	1,176	0.08
Stainless Steel	-105	-102	920	0.1
Graphite	-61	-60	77	0.4
Cold-Rolled Steel	-44	-44	10,152	0.3

(3) Stainless steel generates IM's higher than good conductors such as copper, brass or aluminum but lower than graphite and cold-rolled steel.

(4) Graphite generates very high level of IM's due to nonlinear resistivity.

(5) Cold-rolled steel generates the highest IM level probably due to its nonlinear permeability.

To characterize the IM quantitatively for the standing wave case, we will use the simplest approach of "lumped element" equivalent circuit. A quarter wave open circuited line close to resonance can be approximated by a series RLC circuit. Its input impedance is given by:

$$Z_{in} = R_r + j\chi_r \left(\frac{\omega}{\omega_0} - \frac{\omega_0}{\omega}\right) \tag{5}$$

where

$$R_r = \frac{Z_{0s}}{4} \alpha\lambda \tag{6}$$

$$\chi_r = \omega_0 L = \frac{1}{\omega_0 C} = \frac{\pi Z_{0s}}{4} \tag{7}$$

$$\alpha = \alpha_0 + \alpha_2 I^2 \quad . \tag{8}$$

Nonlinearity terms can get into R and χ through, α, β, and Z_{0s} due to nonlinear surface resistance (resistivity and/or permeability). Close to resonance, the nonlinearity is dominated by R through α. At or close to resonance, the equivalent circuit including the signal source, the IM test fixture and load is given in Figure 4. If current I is flowing through the circuit, the total voltage at the two coupling junctions is given by:

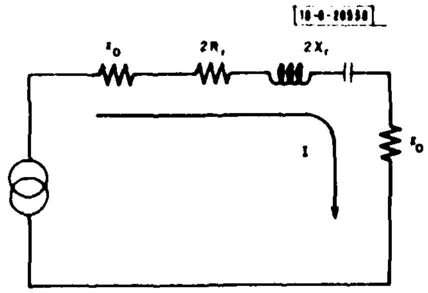

Fig. 4. Equivalent circuit of the IM test fixture close to resonance.

$$V_r = 2R_r I = \frac{\lambda Z_{0s}}{2}\,[\alpha_0 + \alpha_2 I^2 + \ldots]I \quad . \tag{9}$$

If I is $I_1 + I_2$ at frequencies of f_1 and f_2 respectively, the voltage of the third order IM at frequency $(2f_1 \pm f_2)$ is given by:

$$V_{IM} = \frac{3\lambda}{8}\, Z_{0s}\, \alpha_2\, I_1^{\,2}\, I_2 \quad . \tag{10}$$

The detected IM at the load is $(V_{IM}/2)\tau$, where τ is the transmission coefficiency of the IM test fixture. The power ratio of the 3rd order IM to the input power at f_1 is given by:

$$\frac{P_{IM}}{P_{f_1}} = \left(\frac{3\lambda Z_{0s}}{16Z_0}\,\alpha_2\, I_1\, I_2 \tau\right)^2 \quad . \tag{11}$$

For the case of the tested graphite, $P_{IM} = -60$ dBm, $P_{f_1} = 44$ dBm, $I_1 = I_2 = 1$ A, $\lambda = 116$ cm, $\tau = 0.95$, $Z_{0g} = 10\ \Omega$, $Z_0 = 50\ \Omega$. Putting these values into Eqn. (11) we have, $\alpha_2 = 1.46 \times 10^{-6}/A^2$-cm. From the measured insertion loss of 0.4 dB, we calculated $\alpha_0 = 0.78 \times 10^{-2}$ neper/cm, and $\alpha_2/\alpha_0 = 1.86 \times 10^{-4}/A^2$. The second order resistivity to zeroth order resistivity is given by:

$$\frac{\rho_2}{\rho_0} = 2\,\frac{\alpha_2}{\alpha_0}\,(2\pi\delta r_i)^2 \quad . \tag{12}$$

With skin depth $\delta = 1 \times 10^{-2}$ cm, the inner diameter $r_i = 0.2$ cm, we have $\rho_2/\rho_0 = 5.9 \times 10^{-8}$ cm^4/A^2. Compared to good metal conductors like silver (obtained from traveling wave measurement), the relative nonlinearity in resistivity for graphite is more than 7 orders of magnitude higher. Similar calculations for copper, using the measured IM_3 level of -120 dBm and transmission coefficient of 0.99, yield a relative nonlinear resistivity $\rho_2/\rho_0 = 8 \times 10^{-13}$ A^{-2}cm^4. This value is 2 orders of magnitude higher than that of silver previously obtained from long cable measurement and traveling wave analysis. This big difference seems to indicate that the measured IM_3 level of -120 dBm is limited by the test system.

III. DISCUSSION AND CONCLUSIONS

Passive nonlinearities of resistivity in conducting material in contrast with that due to contact junctions were studied by careful measurement and analysis. Forward and backward traveling wave IM's in a long transmission line were distinguished and interpreted. Questions concerning the deviation from Ohm's law by metal conductors were raised and quantitative characterization of the weak nonlinear characteristics of good conductors was attempted. Basic nonlinearity in resistivity was derived from measured IM levels. Numerical results arrived at in the work are exploratory and preliminary in nature. No doubt they will be revised in the future as more measurements are accumulated and better understanding of IM properties are developed. The observed nonlinearity of resistance for a good conductor may be fundamentally related to high current density or it may be due to some secondary processes like temperature or pressure change within an rf cycle.

The demonstration of IM generation by steel, stainless steel, and graphite fiber were conclusive. These materials are used in certain filter and antenna fabrications for low thermal expansion or light weight. Careful design of these components for low IM consideration should be emphasized. The noncontact IM test fixture used in the measurement also suggests a low IM noncontact coaxial connector design for application to a high-power, low-IM transmission path.

The analyses for traveling wave and resonant wave generated IM's can be extended readily to include dielectric nonlinearity effects in the shunt admittance parameter in the transmission line equation. For future interested workers, we suggest an IM study of commonly used dielectrics. If, based on such tests, assurance is obtained that materials such as Teflon and polyethylene do not contribute measureable IM products, confidence in the nonlinearity measurement of good conductors will greatly improve. To use the IM test fixture for good conductors such as copper, brass, and aluminum, test diplexers of lower residual IM's are needed. Especially the contact type connectors used in the test diplexers should be replaced by noncontact types such as those using quarter wavelength coupling.

To measure and characterize weak nonlinearities such as nonlinear resistivity of good conductors, we believe a direct resistivity measurement as a function of current density will be less effective than the indirect IM measurement employed in this work.

REFERENCES

1. W. Shockley, "Hot Electrons in Germanium and Ohm's Law," Bell Syst. Tech. J. 30, 990 (1951).

2. M. A. Heald et al., Plasma Diagnostics with Microwaves (Wiley, New York, 1965).

3. D. E. Foster, "A New Form of Interference-External Cross Modulation," RCA Rev. 1, 18 (1937).

4. Communication Satellites for the 70's: Systems, Edited by N. E. Feldman et al. (M.I.T. Press, Cambridge, Mass., 1971), p. 375.

5. F. S. McCartney, et al., "FLTSATCOM Program Review: Requirements, Design and Performance, EASCON '78 Record, p. 442.

6. R. D. Cox, "Measurements of Waveguide Components and Joint Mixing Products in 6-GHz Frequency Diversity Systems," IEEE Trans. Commun. Tech. COM-18, 33 (1970).

7. R. L. Sicotte et al., "Intermodulation Product and Switching Noise Amplitude of a PIN Diode Switch in the UHF Band," IEEE Trans. Microwave Theory and Tech. MTT-18, 48 (1970).

8. R. M. Kalb et al., "Ferromagnetic Distortion of a Two-Frequency Wave," Bell Syst. Tech. J. 14, 322 (1935).

9. C. E. Young, "An Update on Intermodulation Generation by RF Connector Hardware Containing Ferromagnetic Materials," 9th Annual Connector Symposium Proceedings Cherry Hill, N. J. (October 1976), p. 266.

10. Military Specification MIL-C-26074, Requirements for Chemical Nickel Plating, (November 1956).

11. W. H. Metzger Jr., Symposium on Electroless Nickel Plating, Philadelphia, Pa. (November 1959), p. 16.

12. M. B. Amin et al., "Coaxial Cables as Sources of Intermodulation Interference at Microwave Frequencies," IEEE Trans. on Electromagnetic Compat. EMC-20, 376 (1978).

13. A. Van Hippel, Dielectric Materials and Applications (M.I.T. Press, Cambridge, Mass., 1954), p. 40.

14. G. P. Harnwell, Principles of Electricity and Electromagnetism (McGraw-Hill, New York, 1949), p. 93, p. 148.

15. W. J. Duffin, Electricity and Magnetism (Wiley, New York, 1964), p. 141.

16. E. M. Purcell, Electricity and Magnetism, (McGraw-Hill, New York, 1965), p. 126.

APPENDIX A

RELATIONS BETWEEN NONLINEARITIES IN ATTENUATION AND NONLINEARITIES IN RESISTIVITY PARAMETERS

When the dielectric loss can be neglected, the relation between the attenuation constant and series resistance in a transmission line is given by:

$$\alpha = \frac{R}{2Z_0} \tag{A1}$$

where

$$R = \frac{1}{2\pi}\left(\frac{1}{r_i} + \frac{1}{r_o}\right) R_S$$

$$R_S = \sqrt{\pi f \mu \rho} \quad .$$

The nonlinear resistivity is expressed by a power series expansion:

$$\rho = \rho_0 + \rho_2 J^2 + \rho_4 J^4 + \ldots \tag{A2}$$

The absence of odd order terms implies the medium considered is *assumed* isotropic. For simplicity, in the following we will terminate the above expression at the second term. By combining Eqs. (A1) and (A2), we have:

$$\alpha = \frac{\sqrt{\pi f \mu}}{4\pi Z_0}\left(\frac{\sqrt{\rho_0 + \rho_2 J_i^2}}{r_i} + \frac{\sqrt{\rho_0 + \rho_2 J_o^2}}{r_o}\right)$$

$$= \alpha_0 + \alpha_0 \frac{\rho_2}{2\rho_0} \frac{\left(\frac{J_i^2}{r_i} + \frac{J_o^2}{r_o}\right)}{\left(\frac{1}{r_i} + \frac{1}{r_o}\right)} \equiv \alpha_0 + \alpha_2 I^2 \tag{A3}$$

where

$$\alpha_0 = \frac{\sqrt{\pi f \mu \rho_0}}{4\pi Z_0 r_i} \left(1 + \frac{r_i}{r_o}\right) \quad .$$

From Eq. (A3), we have

$$\alpha_2 I^2 = \frac{\alpha_0 \rho_2}{2\rho_0} \left(\frac{r_o J_i^{\,2} + r_i J_o^{\,2}}{r_i + r_o}\right) \quad . \tag{A4}$$

With the relation $I = J_i 2\pi r_i \delta = J_o 2\pi r_o \delta$, the above equation can be put in the following form:

$$\frac{\alpha_2}{\alpha_0} = \frac{\rho_2}{2\rho_0 (2\pi\delta r_i)^2} \left[\frac{1 + \left(\frac{r_i}{r_o}\right)^3}{1 + \frac{r_i}{r_o}}\right] \quad . \tag{A5}$$

For small $\frac{r_i}{r_o}$, the relation simplifies to:

$$\frac{\alpha_2}{\alpha_0} = \frac{\rho_2}{2\rho_0 (2\pi\delta r_i)^2} \quad . \tag{A6}$$

APPENDIX B

HEURISTIC ANALYSIS OF IM's GENERATED BY TRAVELING WAVES THROUGH A DISTRIBUTED NONLINEARITY

In a transmission line, nonlinearity can be introduced into the system through its characteristic impedance or attenuation and phase "constants". From analysis of the parameters, nonlinear effects due to attenuation "constant" generally dominates. For simplicity, we will concentrate our analysis to this point. Physically the nonlinear attenuation may be due to distributed contact resistance as in a braided coaxial line or due to pure nonlinear skin depth as in a semi-rigid coaxial line. The primary electric voltage variation along the transmission line is given by $V(x) = V_0 e^{-\alpha x}$. The differential change of the above is:

$$dV(x) = -\alpha dxV, \qquad \alpha = \alpha_0 + \alpha_2 V^2 \tag{B1}$$

$$= -\alpha_0 dxV - \alpha_2 dxV^3$$

If $V_0 = V_1 e^{j\omega_1 t} + V_2 e^{j\omega_2 t}$, the differential third order IM voltage with frequency $(2f_1 \pm f_2)$ is given by:

$$dV_{IM_3} = \frac{3}{4} \alpha_2 V_1^2 V_2 dx \tag{B2}$$

Over a section of coaxial line of length ℓ, including the effect of the attenuation on both the fundamental and IM frequencies, the integrated IM voltage in the forward direction is given by:

$$V_{IM_3} = \frac{3V_1^2 V_2}{4} \alpha_2 \int_0^{\ell} e^{-3\alpha_0 x} e^{-(\ell - x)\alpha_0} dx$$

$$= \frac{3V_1^2 V_2 \alpha_2}{8\alpha_0} e^{-\alpha_0 \ell} (1 - e^{-2\alpha_0 \ell}) \tag{B3}$$

Extension of this relation for higher order IM's can be done readily; the results are Eqs. (1) and (2) in the text.

The same result can be obtained by the solution of a non-homogeneous differential equation, which is derived from transmission line equations with two traveling wave excitations. From the equations and also from physical argument, the two fundamental waves and the resulting IM waves all have to travel in the same direction. Otherwise, slow or fast waves will result, which are not supported by the TEM wave line in the frequency range of interest.

APPENDIX C

FORMAL ANALYSIS OF IM's GENERATED BY TRAVELING WAVES IN A TRANSMISSION LINE

Weak nonlinearities encountered in passive IM interference problems allows one to employ a pertubation method of solution. For a uniformly distributed transmission line, the transmission line equations are given by

$$\frac{dV}{dx} = (R + j\omega L)\ I(x) = 0 \tag{C1}$$

$$\frac{dI}{dx} + (G + j\omega C)\ V(x) = 0 \tag{C2}$$

where $(R + j\omega L)$ is a function of I for current induced nonlinearities, and $(G + j\omega C)$ is a function of V for voltage induced nonlinearties.

For the case of nonlinearity due to conducting materials in the transmission line in high frequencies, we can concentrate our attention on the surface resistance, R_S due to skin depth. The nonlinearity of R_S may be due to μ and/or ρ. For simplicity, we will consider the latter case in a coaxial transmission line. Extension of the analysis to include nonlinear μ is straightforward. The series resistance R and R_S are related by:

$$\begin{aligned} R &= \frac{1}{2\pi}\left(\frac{1}{r_o} + \frac{1}{r_i}\right) R_S = \frac{\sqrt{\pi f \mu}}{2\pi}\left(\frac{1}{r_o} + \frac{1}{r_i}\right)\ \rho \\ &= R_0\left[1 + \frac{\rho_2}{2\rho_0} J_o{}^2\right] + R_i\left[1 + \frac{\rho_2}{2\rho_0} J_i{}^2\right] \end{aligned} \tag{C3}$$

where

$$R_o = \frac{\sqrt{\pi f \mu \rho_0}}{2\pi r_o}\ , \tag{C4}$$

$$R_i = \frac{\sqrt{\pi f \mu \rho_0}}{2\pi r_i} \tag{C5}$$

$$\rho = \rho_0 + \rho_2 J^2 \ . \tag{C6}$$

Due to the skin depth effect, an internal inductance L_i term ($\omega L_i = R$) should be added to L. Nonlinearity in ωL_i wil enhance the IM field generated due to R alone by a factor of $\sqrt{2}$. In the following analysis we will neglect the factor for simplicity. The third order nonlinear current term in RI of Equation 1 is given by:

$$R_2 I^3 = \frac{\rho_2}{2} \left[\frac{1}{(2\pi r_o \delta)^3} + \frac{1}{(2\pi r_i \delta)^3}\right] I^3 \ . \tag{C7}$$

The fundamental driving waves which are solutions of the linearized versions of Equations C1 and C2 are called the zero-order solutions for the original equations. The first-order solutions including harmonics and intermodulations of the fundamental waves can be obtained by solving the equations resulting from substitution of the fundamental waves into the original equations, which then has the form of forced oscillation (a nonhomogeneous differential equation).

For $I = I_1 e^{j(\omega_1 t - \beta_1 x)} + I_2 e^{j(\omega_2 t - \beta_2 x)}$, the third order IM driving term at frequency $(2f_1 - f_2)$ is given by

$$-\frac{3}{4} R_2 I_1^2 I_2 e^{-(2\alpha_1 + \alpha_2)x^*} e^{-j(2\beta_1 - \beta_2)x} \ .$$

Equations 1 and 2 can be combined:

$$\frac{d^2}{dx^2} V(x) - \gamma^2 V(x) = \frac{3}{4} R_2 [(2\alpha_1 + \alpha_2) + j(2\beta_1 - \beta_2)] I_1^2 I_2 \, e^{-(2\alpha_1 + \alpha_2)x} e^{-j(2\beta_1 - \beta_2)x}$$

$$\equiv K e^{-(2\alpha_1 + \alpha_2)x} e^{-j(2\beta_1 - \beta_2)x} \tag{C8}$$

*Intuitively, by following the frequency mixing pattern, we might be tempted to use $e^{-(2\alpha_1 - \alpha_2)x}$ factor. But, it would not be right mathematically or physically. Frequency mixing pattern applies only to imaginary exponents representing a real function.

where $\gamma^2 = (R + j\omega L)(G + J\omega C)$.

The general solution for the complementary equation is

$$V_c = A_c\, e^{-\gamma x} + B_c e^{\gamma x} \quad . \tag{C9}$$

Applying the boundary condition $V_c = 0$ for $x = \infty$, we have $B_c = 0$.

For the particular solution for the nonhomogeneous equation, we assume:

$$V_p = A_p\, e^{-\alpha x}\, e^{-j\beta x}$$

$$V_p{}' = -(\alpha + j\beta)\, A_p\, e^{-(\alpha + j\beta)x}$$

$$V_p{}'' = (\alpha + j\beta)^2\, A_p\, e^{-(\alpha + j\beta)x} \quad .$$

Putting the above expressions into Eq. (C8) and equating their coefficients, we have:

$$\begin{aligned} A_p &= \frac{K}{[2\alpha_1+\alpha_2+j(2\beta_1-\beta_2)]^2 - [\bar{\alpha}+j(2\beta_1-\beta_2)]^2} \\ &= \frac{K}{(\alpha^2-\bar{\alpha}^2) + j^2\beta(\alpha-\bar{\alpha})} \\ &\approx \frac{K}{8\bar{\alpha}^2+j4\bar{\alpha}\beta} \end{aligned} \tag{C10}$$

where $\alpha = 2\alpha_1+\alpha_2$, $\beta = 2\beta_1-\beta_2$, and $\gamma = \bar{\alpha}+j(2\beta_1-\beta_2)$ for IM_3 wave are used.

In the last expression, $\bar{\alpha} \approx \alpha_1 \approx \alpha_2$ is assumed.

For simplicity, we will neglect the IM level at x=0. With this initial condition, we have

$$A_c + \frac{K}{8\bar{\alpha}^2 + j4\bar{\alpha}\beta} = 0 \tag{C11}$$

or

$$A_{cr} = \frac{-K}{8\bar{\alpha}^2 + 2\beta^2}$$

$$A_{ci} = \frac{-\beta}{2\bar{\alpha}} A_{cr}$$

$$A_c = A_{cr} + jA_{ci} \quad .$$

And finally, we have

$$V(x) = \left[\frac{-K}{8\bar{\alpha}^2 + 2\beta^2} + \frac{j\beta K}{2\bar{\alpha}(8\bar{\alpha}^2 + 2\beta^2)}\right] e^{-\gamma x} + \frac{K}{8\bar{\alpha}^2 + j4\bar{\alpha}\beta}$$

$$e^{-(2\alpha_1 + \alpha_2)x} \; e^{-j(2\beta_1 - \beta_2)x} \tag{C12}$$

For the case of interest $\beta \gg \bar{\alpha}$, we have

$$V(x) \approx \frac{jK}{4\alpha\beta} \; e^{\bar{\alpha}x} \; (1 - e^{-2\bar{\alpha}x})$$

$$\approx \frac{-3}{16\bar{\alpha}} \; R_2 I_1^{\,2} I_2 \; e^{-\bar{\alpha}x} \; (1 - e^{-2\bar{\alpha}x}) \tag{C13}$$

Recall that

$$\alpha = \frac{R}{2Z_0}$$

$$\alpha V = \frac{RV}{2Z_0} = \frac{RI}{2} = \frac{1}{2} [R_0 I + R_2 I^3]$$

$$\alpha(V_1+V_2) = \alpha_0(V_1+V_2) + \alpha_2(V_1+V_2)^3$$

$$\frac{R}{2}(I_1+I_2) = \frac{1}{2}[R_0(I_1+I_2) + R_2(I_1+I_2)^3] \quad .$$

Compare the 3rd order IM term we have:

$$\frac{3\alpha_2}{4} V_1^2 V_2 = \frac{3R_2}{8} I_1^2 I_2 \quad . \tag{C14}$$

With the relation given by Eq. (C14) we see that the result given by Eq. (C13) agrees with the result given by Eq. (B3) arrived at by a heuristic approach for the same problem.

ACKNOWLEDGMENTS

The author wishes to thank Drs. Leon J. Ricardi and Alan J. Simmons for their interest and advice in the program; Mr. Dennis C. Weikle for his able assistance in setting up the complicated equipment; Mr. John P. McCrillis for his skill and endurance in making the measurements; Mr. Edward B. Murphy for consultation on special material properties; and Ms. Maureen E. Bartlett for her patience in typing and editing the manuscript.

GLOSSARY

A	Ampere
A_n	A Constant
C	Capacitance
E	Electric Field
G	Shunt Conductance
I	Current, I_m Maximum Current
J	Current Density, J_m Maximum Current Density
J_i	Current Density of Inner Conductor of a Coaxial Cable
J_o	Current Density of Outer Conductor of a Coaxial Cable
K_n	A Constant
L	Inductance
L_i	Internal Inductance
P	Power Level
P_{IM}	IM Power Level
P_{f1}	Fundamental Driving Power Level at Frequency f_1
Q_L	Loaded Q of a resonant circuit
R	Series Resistance
R_r	Resistance of a Resonant Circuit
R_s	Surface Resistance
V	Voltage
V_{IM_n}	Nth Order IM Voltage
V_r	Voltage at Resonant Coupling Junction
V_c	Complementary Part of Voltage Solution
V_p	Voltage Particular Solution
V_p'	First Derivative of Voltage Particular Solution
V_p''	Second Derivative of Voltage Particular Solution
V_1	Voltage at f_1
V_2	Voltage at f_2
Z_0	Characteristic Impedance of a Transmission Line
Z_{0s}	Characteristic Impedance of a Resonant Transmission Line Section
Z_{in}	Input Impedance

cm	Centimeter
e	Base of Nature Logarithm
f	Frequency
f_1	Frequency 1
f_2	Frequency 2
f_{IM}	IM Frequency
ℓ	Length of Cable
n	An Odd Number Representing Power Series Order or IM Order
r	Radius of Conductor
r_i	Radius of Inner Conductor
r_o	Radius of Outer Conductor
x	A Length Variable
α	Attenuation Constant
α_0	Attenuation Constant Zeroth Order
α_n	Attenuation Constant nth Order
β	Phase Constant
γ	Complex Propagation Constant
δ	Skin Depth
λ	Wavelength
μ	Permeability of Medium
ρ	Resistivity
ρ_0	Zeroth Order Resistivity
ρ_2	Second Order Resistivity
χ_r	Reactance Slope Parameter of a Resonant Circuit
Ω	Ohm
ω	$2\pi f$, Angular Frequency
ω_o	Angular Resonance Frequency

UNCLASSIFIED

SECURITY CLASSIFICATION OF THIS PAGE (When Data Entered)

REPORT DOCUMENTATION PAGE		READ INSTRUCTIONS BEFORE COMPLETING FORM
1. REPORT NUMBER ESD-TR-79-269	2. GOVT ACCESSION NO.	3. RECIPIENT'S CATALOG NUMBER
4. TITLE (and Subtitle) Intermodulation Measurement in the UHF Band and an Analysis of Some Basic Conducting Materials		5. TYPE OF REPORT & PERIOD COVERED Technical Note 6. PERFORMING ORG. REPORT NUMBER Technical Note 1979-70
7. AUTHOR(s) Joseph C. Lee		8. CONTRACT OR GRANT NUMBER(s) F19628-80-C-0002
9. PERFORMING ORGANIZATION NAME AND ADDRESS Lincoln Laboratory, M.I.T. P.O. Box 73 Lexington, MA 02173		10. PROGRAM ELEMENT, PROJECT, TASK AREA & WORK UNIT NUMBERS Program Element No. 63431F Project No. 2029
11. CONTROLLING OFFICE NAME AND ADDRESS Air Force Systems Command, USAF Andrews AFB Washington, DC 20331		12. REPORT DATE 19 November 1979 13. NUMBER OF PAGES 50
14. MONITORING AGENCY NAME & ADDRESS (if different from Controlling Office) Electronic Systems Division Hanscom AFB Bedford, MA 01731		15. SECURITY CLASS. (of this report) Unclassified 15a. DECLASSIFICATION DOWNGRADING SCHEDULE

16. DISTRIBUTION STATEMENT (of this Report)

Approved for public release; distribution unlimited.

17. DISTRIBUTION STATEMENT (of the abstract entered in Block 20, if different from Report)

18. SUPPLEMENTARY NOTES

None

19. KEY WORDS (Continue on reverse side if necessary and identify by block number)

satellite communication
electromagnetic interference
intermodulation noise
nonlinear resistance
Ohm's law
conducting material
graphite
stainless steel

20. ABSTRACT (Continue on reverse side if necessary and identify by block number)

Intermodulations generated by many commonly used conducting materials were measured in the UHF band and analyzed in terms of resistivity nonlinearities. Contact nonlinearity at the most critical locations in the measurement was avoided by the use of quarter-wavelength couplings. Forward and backward traveling intermodulation waves in a transmission line were distinguished and interpreted. New evidence concerning the deviation from Ohm's law by metal conductors was obtained and quantitative characterization of the weak nonlinear characteristics of good conductors was attempted.

DD FORM 1473 1 JAN 73 EDITION OF 1 NOV 65 IS OBSOLETE

UNCLASSIFIED

SECURITY CLASSIFICATION OF THIS PAGE (When Data Entered)